Graphene Conjugates

DOI: 10.1002/anie.201101351

Graphene Oxide–Peptide Conjugate as an Intracellular Protease Sensor for Caspase-3 Activation Imaging in Live Cells**

Haibo Wang, Qing Zhang, Xia Chu, Tingting Chen, Jia Ge, and Ruqin Yu*

The development of hybrid biological–synthetic nanomaterials for sensing and delivery is of crucial importance for clinical diagnostics and therapeutics.[1] Graphene, a novel one-atom-thick two-dimensional carbon material, in particular has recently attracted great interest for these applications.[2] The unique capacity of graphene or graphene oxide (GO) in adsorbing biomolecules, such as nucleic acids and peptides, with super fluorescence quenching efficiency creates a robust platform for the development of biosensors.[3] Recently, there has been increasing effort in exploiting graphene and GO as fluorescent nanoprobes for intracellular imaging studies. For example, it was demonstrated that nanoscale polyethylene glycol (PEG)-grafted GO may exhibit intrinsic photoluminescence and provide a useful vehicle for cancer-drug delivery and cellular imaging.[4] GO has also been covalently conjugated to a pH-sensitive fluorescent dye through a PEG bridge to serve as a fluorescence sensor for imaging of intracellular pH variations.[5] Efforts toward the construction of intracellular biosensors have recently been reported by using DNA-adsorbing GO nanocomplex for cellular delivery of aptamer and in situ probing of adenosine triphosphate.[6] However, the utility of graphene and GO as intracellular protease sensors for live-cell imaging is still largely unexplored.

Herein, we report the proof-of-principle of a novel intracellular protease sensor based on the nanoconjugate of GO and peptide substrates. Because GO is intrinsically a nanocarrier for delivering peptide cargos inside live cells and a fluorescence quencher for fluorophores adjacent to its surface, the GO–peptide conjugate, after being transported into cells followed by cleavage of the peptide by intracellular proteases, may provide greatly enhanced fluorescence imaging as a result of the release of fluorophores from the GO surface. To test this hypothesis, we chose apoptosis-related caspase-3 activation as the case study. Apoptosis, a mode of programmed cell death, is highly related to many diseases including cancer, neurodegenerative diseases, autoimmune disorders, and heart failure.[7] Caspase-3 has been identified as a central mediator for the initiation and propagation of apoptosis.[8] Consequently, the development of intracellular protease sensors toward caspase-3 is essential for understanding the roles of this protease in physiological and pathological processes as well as for screening the drug candidates for dysregulated apoptosis.[9] Based on intracellular delivery of GO–peptide conjugate and caspase-3-mediated cleavage of substrate peptide, we developed a sensitive, simple, and robust intracellular protease sensor for high-contrast imaging of apoptotic signaling in live cells (Scheme 1 a).

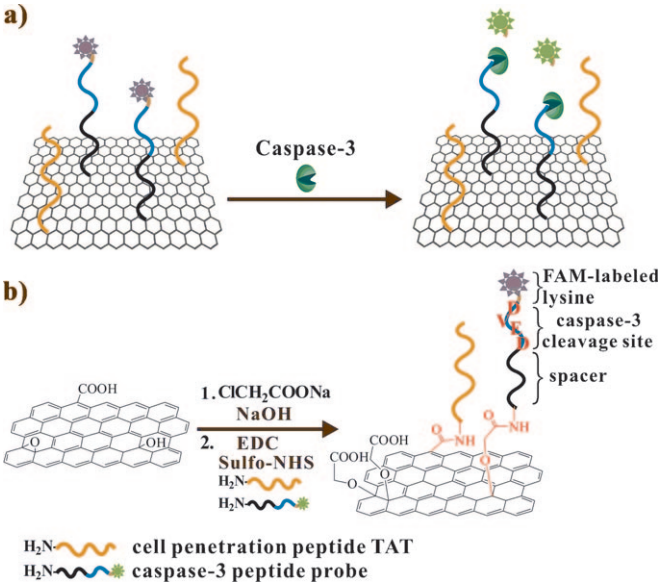

Scheme 1. a) Caspase-3 detection using GO–peptide conjugate. b) Construction of GO–peptide conjugate. EDC = *N*-ethyl-*N*′-[3-(dimethylamino)propyl]carbodiimide hydrochloride, Sulfo-NHS = *N*-hydroxysulfosuccinimide.

To construct an intracellular protease sensor for caspase-3, a peptide probe was designed to comprise at the N terminus a spacer peptide not cleavable by proteases possibly present in cell cultures and the cell interior, a proteolytic moiety DEVD (Asp-Glu-Val-Asp) peptide sequence,[10] and fluorescein amidite (FAM)-labeled lysine at the C terminus (Scheme 1 b). Because synthetic peptides were reported to be assembled on GO surfaces with certain affinity,[3e,f] we initially prepared a noncovalent complex of GO–peptide by using a simple self-assembly procedure: incubation of peptides with GO to allow self-assembly of the peptides on GO surfaces. However, we found that such a GO–peptide composite showed substantially enhanced fluorescence upon incubation

[*] Dr. H. Wang, Dr. Q. Zhang, Prof. Dr. X. Chu, Dr. T. Chen, Dr. J. Ge, Prof. R. Yu
State Key Laboratory of Chemo/Bio-Sensing and Chemometrics, College of Chemistry and Chemical Engineering, Hunan University, Changsha 410082 (China)
Fax: (+86) 731-8882-1916
E-mail: xiachu@hnu.edu.cn

[**] This work was supported by the NSFC (20975035), "973" National Key Basic Research Program (2007CB310500), and PCSIRT.

Supporting information for this article is available on the WWW under http://dx.doi.org/10.1002/anie.201101351.

with cell growth medium (Figure S1 in the Supporting Information). We ascribed the effect to the weak affinity of peptides to GO such that peptides adsorbed on GO surfaces were displaced by proteins present in the cell growth medium.[11] Titration of the GO–peptide composite with a common growth-medium component, bovine serum albumin (BSA), confirmed this speculation (Figure S2 in the Supporting Information), thus implying that the noncovalent complex of GO–peptide was unstable in protein-abundant media.

Covalent conjugation of the peptide probe and GO was then chosen for constructing the intracellular protease sensor for caspase-3 (Scheme 1b). To increase the carboxylic acid groups on the GO surface for peptide conjugation, we treated GO with chloroacetic acid under strongly basic conditions to activate epoxide and ester groups and to convert hydroxyl groups to carboxylic acid moieties.[4] Subsequently, the peptide probe together with a cell penetration peptide TAT (2:1 molar concentration ratio) was conjugated to GO using the succinimide coupling (EDC–NHS) method to obtain the GO–peptide conjugate.[12] The cell penetration peptide TAT was used to improve the efficiency of intracellular delivery and endosomal escape of the GO–peptide conjugate.[13]

The resulting GO–peptide conjugate was found to give very weak fluorescence, which confirmed the highly efficient fluorescence quenching of the fluorescein label by GO. Moreover, covalent coupling of GO and peptides furnished the conjugate with desirable stability in cell growth medium, with only slight fluorescence enhancement observed in the medium and in BSA titration (Figures S1 and S2 in the Supporting Information). Such slight fluorescence enhancement might be attributable to conformational changes of the peptide probes due to protein adsorption on GO surfaces. As a result, we introduced BSA (0.5 mg mL^{-1}) to the solution of GO–peptide conjugate for further experiments. Presumably, this could facilitate saturated protein adsorption on GO surfaces, thus eliminating possible fluorescence alterations of the conjugate upon adding protein-abundant media.

The GO–peptide conjugate was characterized by atomic force microscopy (AFM) to provide its morphological profile. After sonication treatment, the GO sheets mostly had a lateral width of less than 200 nm (Figure S3 in the Supporting Information) with a topological height of 1–2 nm (Figure 1a), which was typical for single- or double- layered sheets of GO.[14] The GO–peptide conjugate had a topological height of over 5 nm across the lateral dimension (Figure 1b), which implied high coverage of peptides on the GO–peptide conjugate surfaces.

The chemical structures of GO and GO–peptide conjugate were further confirmed by infrared spectroscopy (Figure S4 in the Supporting Information). The appearance of characteristic absorption peaks at 3400, 1700, and 1580 cm^{-1} (stretching vibrations of −OH, C=O, and C=C, respectively) revealed the presence of −OH, C=O and C=C functional groups in GO. After chloroacetic acid activation, the resulting GO derivative showed a stronger absorption band at 1630 cm^{-1}, indicative of the formation of carboxylate moieties COO^-. After conjugation of peptides with GO, a strong characteristic band appeared at 1650 cm^{-1} (stretching vibration of −CO−NH−) with an increased small peak near 2900 cm^{-1} (stretching vibration of $-CH_2$), which indicated the successful formation of GO–peptide conjugate.

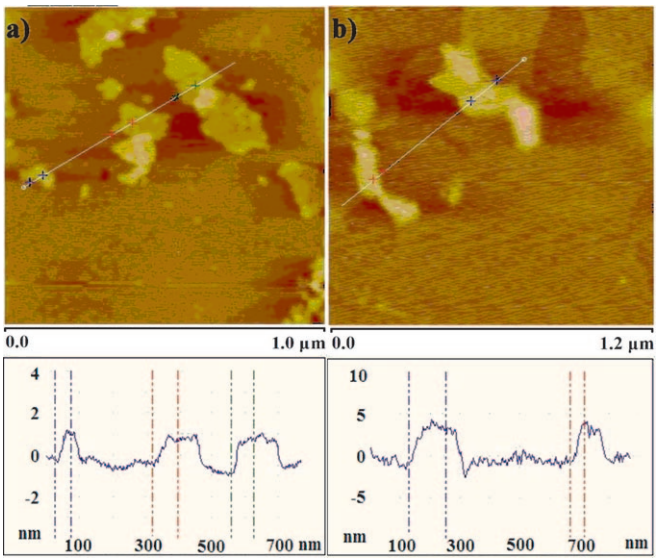

Figure 1. AFM images (top) and height profiles (bottom) of a) GO and b) GO–peptide conjugate.

In addition, the resulting GO–peptide conjugate exhibited excellent solubility and stability in water and cell growth medium (Figure S5 in the Supporting Information). This favorably supported the potential of GO–peptide conjugate for in vitro assay and intracellular imaging applications. Interestingly, the suspensions of GO and GO–peptide conjugate were found to display clearly different colors, GO–peptide conjugate being much darker than GO. This color change might be attributable to the restoration of electronic conjugation within the GO sheet through opening of epoxide and hydrolysis of ester groups under the strongly basic conditions employed during chloroacetic acid treatment of GO.[4] Taken together, these data provided immediate evidence for the successful preparation of the GO–peptide conjugate.

We then investigated the capabilities of the GO–peptide conjugate as a protease sensor for in vitro assay of caspase-3 activity. Mixtures of GO–peptide conjugate and protease were prepared and incubated at 37 °C. The fluorescence spectra were measured in the range from 500 to 620 nm after 60 min of incubation (Figure 2a). It was found that the GO–peptide conjugate gave fluorescence spectra with insignificant difference in the buffer and the cell growth medium. This verified that the introduction of BSA into the GO–peptide conjugate suspension avoided alterations of the fluorescence background caused by protein-abundant media. The presence of caspase-3, as expected, gave a strong fluorescence peak for the conjugate of GO with caspase-3-specific substrate peptide DEVD, which suggested that this GO–peptide conjugate could act as a sensor for caspase-3 with desirable "signal-on" architecture. In contrast, the GO–peptide conjugate did not display any appreciable fluorescence activation in the presence of caspase-2, a protease with negligible cleavage to the peptide substrate DEVD.[15] Additionally, in the presence of Z-DEVD-fluoromethylketone (FMK), a strong caspase-3

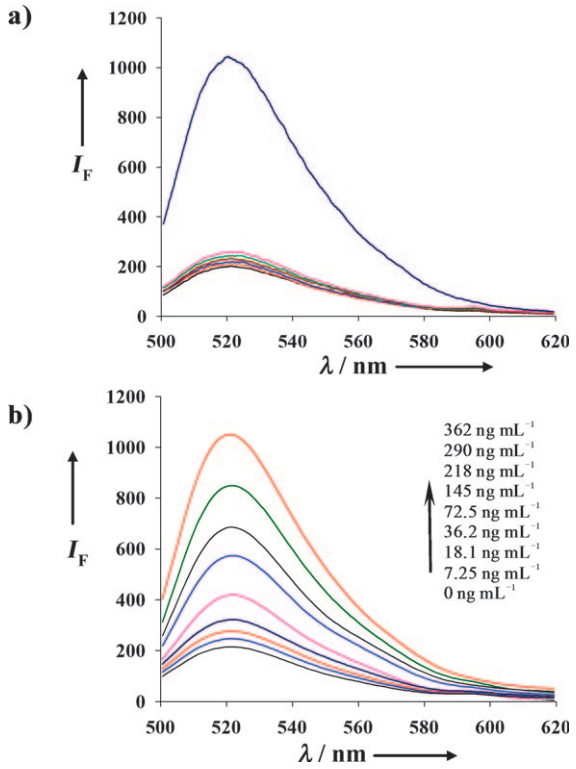

Figure 2. a) Fluorescence intensity (I_F) spectra for the conjugate of GO with caspase-3-specific substrate peptide DEVD in buffer (red), cell growth medium (black), caspase-3 (dark blue), caspase-2 (blue), and inhibitor Z-DEVD-FMK (100 μM) plus caspase-3 (brown), and for the conjugate of GO with nonspecific substrate peptide DEVG in buffer (green) and caspase-3 (pink). Concentration of caspase-3 and -2: 362 ng mL^{-1}. b) Fluorescence spectral responses of the conjugate of GO with caspase-3-specific substrate peptide to caspase-3 of varying concentrations.

inhibitor, only a very weak fluorescence spectrum was obtained after incubating the GO–peptide conjugate with caspase-3, thereby implying that the protease sensor was viable for inhibitor assays. On the other hand, we performed another control experiment using the conjugate of GO with nonspecific peptide substrate, DEVG,[16] which also only gave insignificant enhancement of fluorescence in the presence of caspase-3. These findings, therefore, validated the specificity of the protease sensor for caspase-3 detection.

Next, we performed assays using mixtures of GO–peptide conjugate and caspase-3 of varying concentrations to demonstrate the quantitative nature of the protease sensor (Figure 2b). The fluorescence peaks dynamically increased with increasing caspase-3 concentration in the range from 7.25 to 362 ng mL^{-1}. A plot of fluorescence at the maximum emission wavelength of 520 nm versus caspase-3 concentration revealed a linear response characteristic of the protease sensor, with a readily achieved detection limit of 7.25 ng mL^{-1} (ca. 0.4 nM; Figure S6 in the Supporting Information).

Further inspection of the protease sensor was performed by using fluorescence anisotropy assay and time-dependent fluorescence measurements at the maximum emission wavelength of 520 nm. In response to caspase-3, the protease sensor displayed a significantly decreased fluorescence anisotropy profile, revealing a substantial loss of molecular weight of the fluorophore and thereby evidencing proteolytic cleavage and release of fluorophores from the GO–peptide conjugate. No appreciable alterations were obtained in control experiments using inhibitor-inactivated caspase-3 or another protease (caspase-2), which confirmed that the protease sensor was highly specific to caspase-3 activation (Figure S7 in the Supporting Information). Likewise, the time-dependent response profile also showed insignificant fluorescence activation in control experiments using inhibitor-inactivated caspase-3 or a nonspecific protease incubated with the GO–peptide conjugate (ca. 0.07 mg mL^{-1}). The presence of caspase-3 (362 ng mL^{-1}), however, triggered a rapid fluorescence activation process, which indicated that the protease sensor allowed real-time detection of caspase-3 activity (Figure S8 in the Supporting Information).

After interrogating the response characteristics of the protease sensor in vitro, we then explored its potential for live-cell imaging of caspase-3 activation. Human cervix carcinoma (HeLa) cells were incubated with GO–peptide conjugate, noncovalent complex of GO–peptide, GO, or a mixture of fluorescein-labeled substrate peptide with cell penetration peptide TAT (2:1 molar ratio) in the cell growth medium for 8 h at 37 °C. Then, the cells were treated with staurosporine (STS, 4 μM), a commonly used apoptosis inducer,[9b,d] for another 4 h. As shown in Figure 3, cells incubated with GO or peptide mixture did not give appreciable contrast in the fluorescence images, thereby indicating that GO was not fluorescent in the detection window and the fluorophore-labeled peptide was unable to be taken up by HeLa cells. Surprisingly, no remarkable fluorescence contrast

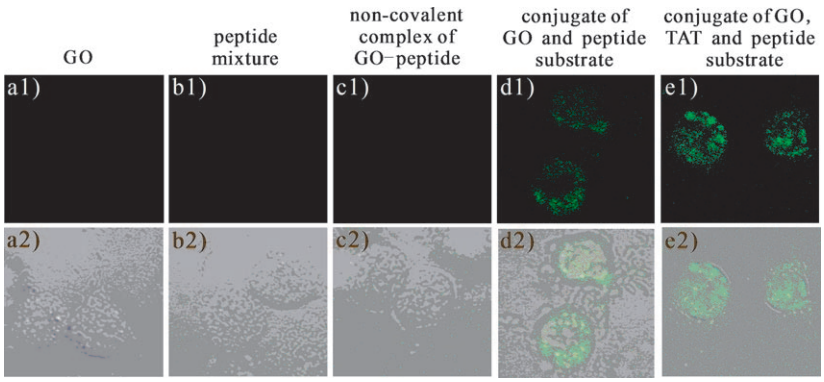

Figure 3. Confocal fluorescence microscopy images of HeLa cells treated with 4 μM STS for 4 h after incubating with a) GO, b) 1.5 mM mixture of fluorescein-labeled caspase-3-specific substrate peptide and cell penetration peptide TAT, c) noncovalent complex of GO–peptide, d) conjugate of GO and substrate peptide, and e) conjugate of GO, TAT, and substrate peptide, for 8 h at 37 °C in cell growth medium. Concentration of GO, complex, and conjugates: 70 μg mL^{-1}. 1) Fluorescence images; 2) overlap of fluorescence and bright-field images.

was obtained in the image for cells incubated with noncovalent complex of GO–peptide. This implied that the noncovalent complex of GO–peptide could not serve as an efficient carrier to deliver peptides into cells, presumably because of desorption of peptides from the GO surface.

In contrast, an activated fluorescence image was obtained for the cells incubated with conjugates of GO and substrate peptide, which indicated that GO–peptide conjugate could enter and internalize into cells by itself and sense caspase-3 activation induced by STS. Interestingly, a brighter green fluorescence image was obtained for the cells incubated with conjugates of GO, TAT peptide, and substrate peptide, which suggested that TAT peptide-modified GO–peptide conjugate could be more efficiently delivered into HeLa cells. Presumably, the delivery of TAT-unmodified GO–peptide conjugate into cells might result from lysosomal permeabilization during apoptosis. The improved delivery efficiency of TAT-modified GO–peptide conjugate might be a function of both TAT-induced endosomal escape and lysosomal permeabilization.[9a]

To validate whether the fluorescence signal was specific to caspase-3 activation, we further performed experiments using varying STS concentrations, conjugate of GO with nonspecific substrate peptide, or caspase-3 inhibitor. As shown in Figure 4, with increasing STS concentration, brighter fluorescence images were achieved with the cells incubated with conjugate of GO with caspase-3-specific peptide, thereby evidencing direct correlation of intracellular fluorescence activation to STS-induced apoptosis. With cells treated using STS together with Z-DEVD-FMK, we did not obtain obvious fluorescence contrast, which confirmed the specificity of our live-cell imaging strategy to caspase-3 activation. The conjugate of GO with nonspecific peptide, DEVG, also did not yield noticeable fluorescence contrast for cells treated with STS. This substrate specificity further indicated that the fluorescence activation in cells was specific to caspase-3 activation. On the other hand, we performed assays of caspase-3 activity in extracts of the corresponding batch of cells using a Caspase-3 Colorimetric Assay Kit (Figure S9 in the Supporting Information). The data also revealed that caspase-3 activity was elevated in cells treated with increasing STS concentrations, and caspase-3 activity was very low in the presence of inhibitor. These results were in good consistency with those obtained in the live-cell imaging experiments.

To further verify the internalization of GO–peptide conjugate in HeLa cells, *Z*-scanning confocal imaging was performed (Figure S10 in the Supporting Information). It was clear that bright fluorescence was present throughout the whole cells, which suggested efficient delivery of the GO–peptide conjugate in the cytosol. This revealed that the GO–peptide conjugate afforded a robust intracellular protease sensor for high-contrast imaging of caspase-3 activation in live cells.

In conclusion, we have presented a novel graphene-based strategy to develop intracellular protease sensors for live-cell imaging based on covalent conjugation of GO and peptide substrates with fluorophore labels. Compared with the nowadays prevailing strategy of noncovalent assembly for graphene-based biosensor construction, the use of a covalent conjugate eliminated effectively the displacement of peptide probes caused by protein adsorption, thus substantially improving the stability of protease sensors in protein-abundant media. The strategy was demonstrated using the apoptosis-related caspase-3 activation system. In vitro assays revealed that the GO–peptide conjugate provided a robust, sensitive, and selective sensor for quantitative detection of caspase-3. Confocal fluorescence microscopy experiments with HeLa cells suggested that the GO–peptide conjugate was efficiently delivered into live cells and acted as a "signal-on" intracellular sensor for specific, high-contrast imaging of caspase-3 activation. Considering the high quenching efficiency of GO to varying fluorescent labels and the tremendous importance of proteases, the developed strategy could be immediately extended to multiplex in vitro assays or live-cell imaging of multiple proteases by use of the conjugate of GO to different peptide substrates with multicolor fluorophore tags (Figure S11 in the Supporting Information). In view of these advantages, this new GO–peptide conjugate-based strategy for developing robust protease sensors is expected to hold great potential for in vitro and live-cell applications in medical research and clinical diagnostics.

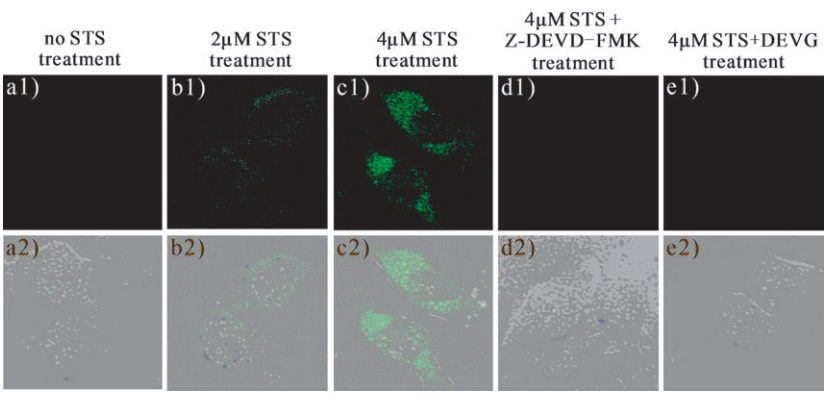

Figure 4. Confocal fluorescence microscopy images of HeLa cells treated with a) no STS, b) 2 μM STS, c) 4 μM STS, d) 4 μM STS and 100 μM inhibitor Z-DEVD-FMK for 4 h after incubating with conjugate of GO and caspase-3-specific peptide, and e) treated with 4 μM STS for 4 h after incubating with conjugate of GO and nonspecific peptide substrate DEVG. 1) Fluorescence images; 2) overlap of fluorescence and bright-field images.

Received: February 23, 2011
Revised: April 8, 2011
Published online: June 16, 2011

Keywords: biosensors · caspase · fluorescent probes · graphene · peptides

[1] D. A. Giljohann, D. S. Seferos, W. L. Daniel, M. D. Massich, P. C. Patel, C. A. Mirkin, *Angew. Chem.* **2010**, *122*, 3352 – 3366; *Angew. Chem. Int. Ed.* **2010**, *49*, 3280 – 3294.

[2] a) D. R. Dreyer, R. S. Ruoff, C. W. Bielawski, *Angew. Chem.* **2010**, *122*, 9524 – 9532; *Angew. Chem. Int. Ed.* **2010**, *49*, 9336 – 9344; b) C. N. R. Rao, A. K. Sood, K. S. Subrahmanyam, A. Govindaraj, *Angew. Chem.*

2009, *121*, 7890 – 7916; *Angew. Chem. Int. Ed.* **2009**, *48*, 7752 – 7777.

[3] a) J. Balapanuru, J.-X. Yang, S. Xiao, Q. Bao, M. Jahan, L. Polavarapu, J. Wei, Q.-H. Xu, K. P. Loh, *Angew. Chem.* **2010**, *122*, 6699 – 6703; *Angew. Chem. Int. Ed.* **2010**, *49*, 6549 – 6553; b) C.-H. Lu, H.-H. Yang, C.-L. Zhu, X. Chen, G.-N. Chen, *Angew. Chem.* **2009**, *121*, 4879 – 4881; *Angew. Chem. Int. Ed.* **2009**, *48*, 4785 – 4787; c) H. Jang, Y.-K. Kim, H.-M. Kwon, W.-S. Yeo, D.-E. Kim, D.-H. Min, *Angew. Chem.* **2010**, *122*, 5839 – 5843; *Angew. Chem. Int. Ed.* **2010**, *49*, 5703 – 5707; d) J. H. Jung, D. S. Cheon, F. Liu, K. B. Lee, T. S. Seo, *Angew. Chem.* **2010**, *122*, 5844 – 5847; *Angew. Chem. Int. Ed.* **2010**, *49*, 5708 – 5711; e) X. Wang, C. Wang, K. Qu, Y. Song, J. Ren, D. Miyoshi, N. Sugimoto, X. Qu, *Adv. Funct. Mater.* **2010**, *20*, 3967 – 3971; f) M. Zhang, B.-C. Yin, X.-F. Wang, B.-C. Ye, *Chem. Commun.* **2011**, *47*, 2399 – 2401.

[4] a) Z. Liu, J. T. Robinson, X. Sun, H. Dai, *J. Am. Chem. Soc.* **2008**, *130*, 10876 – 10877; b) X. Sun, Z. Liu, K. Welsher, J. T. Robinson, A. Goodwin, S. Zaric, H. Dai, *Nano Res.* **2008**, *1*, 203 – 212.

[5] C. Peng, W. Hu, Y. Zhou, C. Fan, Q. Huang, *Small* **2010**, *6*, 1686 – 1692.

[6] Y. Wang, Z. Li, D. Hu, C.-T. Lin, J. Li, Y. Lin, *J. Am. Chem. Soc.* **2010**, *132*, 9274 – 9276.

[7] F. H. Igney, P. H. Krammer, *Nat. Rev. Cancer* **2002**, *2*, 277 – 287.

[8] D. R. Green, *Cell* **1998**, *94*, 695 – 698.

[9] a) Y.-W. Jun, S. Sheikholeslami, D. R. Hostetter, C. Tajon, C. S. Craik, A. P. Alivisatos, *Proc. Natl. Acad. Sci. USA* **2009**, *106*, 17735 – 17740; b) S.-Y. Lin, N.-T. Chen, S.-P. Sun, J. C. Chang, Y.-C. Wang, C.-S. Yang, L.-W. Lo, *J. Am. Chem. Soc.* **2010**, *132*, 8309 – 8315; c) K. Kim, M. Lee, H. Park, J.-H. Kim, S. Kim, H. Chung, K. Choi, I.-S. Kim, B. L. Seong, I. C. Kwon, *J. Am. Chem. Soc.* **2006**, *128*, 3490 – 3491; d) A. Kanno, Y. Yamanaka, H. Hirano, Y. Umezawa, T. Ozawa, *Angew. Chem.* **2007**, *119*, 7739 – 7743; *Angew. Chem. Int. Ed.* **2007**, *46*, 7595 – 7599.

[10] X. Xu, A. L. V. Gerard, B. C. B. Huang, D. C. Anderson, D. G. Payan, Y. Luo, *Nucleic Acids Res.* **1998**, *26*, 2034 – 2035.

[11] J. Liu, S. Fu, B. Yuan, Y. Li, Z. Deng, *J. Am. Chem. Soc.* **2010**, *132*, 7279 – 7281.

[12] a) Y. Huang, Y.-L. Zhang, X. Xu, J.-H. Jiang, G.-L. Shen, R.-Q. Yu, *J. Am. Chem. Soc.* **2009**, *131*, 2478 – 2480; b) Z. Wu, Z. Zhen, J.-H. Jiang, G.-L. Shen, R.-Q. Yu, *J. Am. Chem. Soc.* **2009**, *131*, 12325 – 12332.

[13] J. M. de la Fuente, C. C. Berry, *Bioconjugate Chem.* **2005**, *16*, 1176 – 1180.

[14] Z. Luo, Y. Lu, L. A. Somers, A. T. C. Johnson, *J. Am. Chem. Soc.* **2009**, *131*, 898 – 899.

[15] R. V. Talanian, C. Quinlan, S. Trautz, M. C. Hackett, J. A. Mankovich, D. Banach, T. Ghayur, K. D. Brady, W. W. Wong, *J. Biol. Chem.* **1997**, *272*, 9677 – 9682.

[16] M. Rehm, H. Dubmann, R. U. Janicke, J. M. Tavare, D. Kogel, J. H. M. Prehn, *J. Biol. Chem.* **2002**, *277*, 24506 – 24514.

